physchem

Article

Control of Self-Assembly of Amphiphilic Wedge-Shaped Mesogens Using a Combination of Magnetic Field and Temperature Treatment

Denis V. Anokhin [1,2,3,*], Ludmila L. Gur'eva [2], Kseniia N. Grafskaia [2,4], Evgeniy S. Pikalov [2,3], Ainur F. Abukaev [2,5], Viktor P. Tarasov [2] and Dimitri A. Ivanov [1,2,3,6]

[1] Center for Genetics and Life Science, Sirius University of Science and Technology, 1 Olympic Ave, 354340 Sochi, Russia
[2] Institute of Chemical Physics Problems of RAS, Acad. Semenov Av., 1, 142432 Chernogolovka, Russia
[3] Chemical Department, Lomonosov Moscow State University, Leninskie Gory, 1, 119991 Moscow, Russia
[4] Institute of Condensed Matter and Nanosciences, Université catholique de Louvain (UCLouvain), Croix du Sud 1, Box L7.04.02, 1348 Louvain-la-Neuve, Belgium
[5] School of Electronics, Photonics and Molecular Physics, Moscow Institute of Physics and Technology (National Research University), Institutsky per. 9, 141700 Dolgoprudny, Russia
[6] Institut de Sciences des Matériaux de Mulhouse-IS2M, CNRS UMR 7361, Jean Starcky, 15, F-68057 Mulhouse, France
* Correspondence: deniano@yahoo.com

Citation: Anokhin, D.V.; Gur'eva, L.L.; Grafskaia, K.N.; Pikalov, E.S.; Abukaev, A.F.; Tarasov, V.P.; Ivanov, D.A. Control of Self-Assembly of Amphiphilic Wedge-Shaped Mesogens Using a Combination of Magnetic Field and Temperature Treatment. *Physchem* **2022**, *2*, 274–285. https://doi.org/10.3390/physchem2030020

Academic Editor: Jacinto Sá

Received: 3 July 2022
Accepted: 7 August 2022
Published: 3 September 2022

Publisher's Note: MDPI stays neutral with regard to jurisdictional claims in published maps and institutional affiliations.

Copyright: © 2022 by the authors. Licensee MDPI, Basel, Switzerland. This article is an open access article distributed under the terms and conditions of the Creative Commons Attribution (CC BY) license (https://creativecommons.org/licenses/by/4.0/).

Abstract: The report elucidates for the first time a significant effect of a strong magnetic field combined with thermal treatment on the texture of thin liquid-crystalline films in a smectic state. The metastable texture generated in the magnetic field was arrested via the crystallization of mesogens while they cooled to room temperature. The effect was demonstrated on a series of wedge-shaped amphiphilic mesogens based on 1,2,3-tris-(dodecyloxy)benzene (TDOB): asymmetric 2,3,4-tris-(dodecyloxy)benzenesulfonic acid (TDOBSH) and its sodium (TDOBSNa) and pyridine (TDOBSPyr) salts. The thermotropic properties and the structure of the liquid crystal phases of the synthesized compounds were studied using differential scanning calorimetry, polarized optical microscopy and X-ray diffraction. It was shown that, depending on the type of counterion, the synthesized mesogens formed different supramolecular structures. The largest effect of the intense magnetic field was observed for the pyridine salt for which an ordered primitive cubic phase texture was generated upon the normal application of the magnetic field with respect to the film. In contrast, for the corresponding acid, an improvement of the gyroid cubic phase orientation was detected with the magnetic field oriented along the film. A highly ordered columnar phase of the sodium salt was affected only minimally by the magnetic field.

Keywords: wedge-shaped amphiphilic mesogens; 2,3,4-tris-(dodecyloxy)benzene sulfonates; orientation in magnetic field; differential scanning calorimetry; grazing-incidence X-ray diffraction

1. Introduction

One of the most powerful tools employed for the development of smart, sensitive materials is molecular self-assembly [1]. The unique properties of supramolecular structures include spontaneous formation and easy transformation under the influence of external factors (temperature, pressure, chemical environment, irradiation, magnetic and electric fields, etc.) due to the dynamic nature of weak intermolecular bonds, which are susceptible to electrostatic, van der Waals or hydrogen interactions. The structure of such molecular "building blocks" is determined both by the shape and size of the original molecules and the position of functional groups [2]. External factors shift the balance of these interactions, stimulating a change in molecular conformation and, consequently, a phase transition to a new structure. In particular, the application of a magnetic field could in some instances generate a texture that would be thermodynamically unstable—and therefore not easily achievable in the absence of the field—such as the so-called homeotropic orientation which will be discussed later.

Wedge-shaped amphiphilic mesogens based on tris(alkyloxy)benzene sulphonic acid are a relatively new class of self-assembling molecules [3,4]. They can serve as building blocks for the synthesis of novel functional materials, such as highly regular polymeric ion-conductive membranes, nanoreactors and drug delivery systems. The variation of chemical composition (change in alkyl chain length, substitution of counterion, addition of azobenzene group) and external factors (temperature change, presence of saturated solvent vapor atmosphere with different polarity, UV-irradiation) allow them to form crystalline or liquid-crystalline phases of different symmetry.

The self-assembly of amphiphilic mesogens seems a promising "bottom-up" approach for the fabrication of membranes with a highly defined size and topology of ion channels, which could become an alternative to Nafion or zeolites as an efficient proton-conductive membrane for the application of perspective fuel cells [5–7]. The proton transport across the membranes built from such molecules can be optimized using external stimuli during film preparation [8]. The most common mesophase structures for thin films of mesogens containing ion channels are columnar (hexagonal and monoclinic) and smectic. Such liquid-crystalline films exhibit textures which mainly have in-plane orientated channels, which is not optimal for proton transport across the membrane. To achieve optimal membrane efficiency, it is necessary to increase the number of channels for proton transport across the membrane, which is possible when the channels are normally, or homeotropically, oriented with respect to the membrane film surface. However, the ability to switch the orientation of the channels to normal or homeotropic is limited by the thermodynamic instability of the texture [9–11]. One of the ways to ensure a stable homeotropic texture in thin films is to apply a magnetic field to the mesogens in an isotropic or liquid-crystalline (LC) state and then fix it through chemical bonding [12–15]. The membranes based on polymerizable wedge-shaped amphiphilic LCs were shown to form highly ordered mesophases when under the effect of a magnetic field, resulting in an increase in their conductivity by two orders of magnitude compared to unoriented materials [15]. It is important to mention that the reorientation of mesogens by exposure to a magnetic field mainly occurs in a nematic LC state which is characterized by a low degree of molecular ordering. For columnar phases, a magnetic field was found only to enhance the thermodynamically stable planar orientation [15].

Derivatives of symmetric [4,16–18] and asymmetric [3,19–22] tris(alkyloxy)benzenesulfonic acid exhibit a variety of both crystalline and thermotropic liquid-crystalline mesophases, including smectic, cubic, ordered and disordered columnar mesophases [19–22]. These phases can be stabilized by physical and chemical cross-linking to form polymer membranes with well-controlled ion channel topologies [4,8].

In summary, the development of approaches to control the orientation of ion-conducting channels in self-organized systems of wedge-shaped amphiphilic LC compounds is of great interest [3,4,8,16–22]. In the present work, a combined effect of high-temperature annealing and magnetic field exposure was studied for wedge-shaped amphiphilic mesogens: namely, asymmetric 2,3,4-tris-(dodecyloxy)benzenesulfonic acid (TDBOSH) as well as its sodium (TDBOSNa) and pyridine (TDBOSPyr) salts. These compounds demonstrate complex thermotropic behavior with the formation of both crystalline and liquid-crystalline phases. As such, this study opens avenues for the design of thin films with unusual textures by applying strong external stimuli like magnetic fields on the films in an LC state with high molecular mobility and following up by adjusting to the desired supramolecular morphology via crystallization at room temperature.

2. Materials and Methods

2.1. Synthesis

The TDBOSH, TDBOSNa and TDBOSPyr were synthesized according to the following Scheme 1 by the methods described in [4,19–22]:

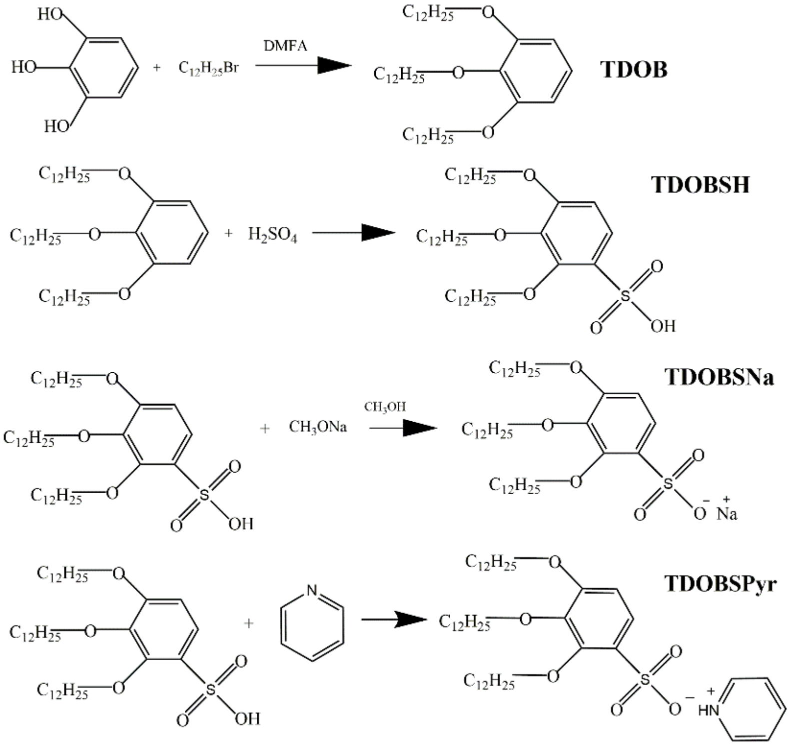

Scheme 1. Synthesis of TDOB, TDBOSH, TDBOSNa and TDBOSPyr.

2.2. Reagents

Pyrogallol (99%), 1-bromodododecane (95%), pyridine (99.8%), sodium methylate (pure, anhydrous) (Sigma-Aldrich, St. Louis, MI, USA), benzene (Cd, Ecos), acetone, sulphuric acid and potassium carbonate (CH, Chemmed) were used without further purification. Molecular sieves 4A (granules, diameter 3.2 mm, Acros Organics, Geel, Belgium) were calcinated under vacuum at 250 °C. Dimethylformamide (DMFA) (99.8%, Sigma-Aldrich) was dehydrated by azeotropic distillation with benzene at atmospheric pressure, and incubated over molecular sieves 4A for 3 days, followed by vacuum distillation under argon current. The methanol (Cr, Chemmed) for recrystallization was distilled over molecular sieves 4A.

2.3. Methods of the Analysis

The identification of the synthesized compounds was carried out by IR, ^{1}H NMR and ^{13}C NMR spectroscopy and elemental analysis. IR spectra were taken in KBr tablets using a Specord M80 spectrometer with Soft Spectra software. Two-dimensional Cosy and HSQC NMR spectra were measured in $CDCl_3$ solution with a trimethylsilane (TMS) reporter on an AVANCE-III-500 spectrometer and were interpreted using Mest ReNova 12-0-0 Manual software. The elemental analysis was performed on Vario EL cube equipment (Elementar GmbH, Langenselbold, Germany).

The thermotropic properties of compounds were determined by the differential scanning calorimetry (DSC) methods using a “DSC 30 Mettler Toledo Star System” in the temperature range from −40 to 140 °C with a scanning rate of 5 deg/min. In order to check the reversibility of phase transitions, two DSC heating-cooling ramps were performed for all samples.

Thin films (200–500 nm) for POM and GIXD experiments were prepared by the spin-coating of 10 mg/mL solution in chloroform on a silicon substrate at a rate of 1000 rpm. For NMR experiments the samples were prepared by the drop-casting of 20 mg/mL solution in chloroform on a silicon substrate. Then the drop-casted films were annealed at 85 °C for 1 h in a vacuum oven.

The effect of thermal history on the texture of the thin films of the synthesized compounds was studied using polarized optical microscopy (POM). The spin-coated films were annealed in a normal atmosphere at 85 °C for 3 h using a Linkam LTS420 thermal stage. Optical measurements of the as-cast and annealed films were carried out with a Karl Zeiss Axio Scope A1Pol microscope in polarized light.

The structure of unoriented samples was studied by X-ray diffraction (XRD) on a custom-built WAXS/SAXS X-ray System diffractometer with a 1.54 Å wavelength equipped with a two-dimensional Pilatus 300k detector. The sample-detector distance was 1.15 m. The modulus of the scattering vector **s** ($|\mathbf{s}| = 2\sin\vartheta/\lambda$, where ϑ is the Bragg angle, λ is the wavelength and $|\mathbf{s}|$ is the norm of the **s** vector) was calibrated using several diffraction orders of silver behenate. To exclude the influence of humidity, the measurements were carried out in vacuum. The analysis of X-ray data, including background subtraction and the radial integration of 2D diffractograms, was performed with procedures developed in the IgorPro (Wavemetrics Ltd., Lake Oswego, OR, USA) environment.

To address the effect of the magnetic field (MF) on the thin film texture, the capillary with sample on substrate was placed into the resonator of the BRUKER-500 NMR spectrometer (proton frequency 400 MHz). The magnetic induction 9.5 Tesla was oriented normal to the capillary axis. As was shown in [15], such intensity is sufficient for the reorganization of benzene-containing molecules in LC phase. The orientation of the **B** vector of MF to set it normal (Figure 1a) or parallel (Figure 1b) to the film surface was achieved by rotating the capillary around its axis. Then, the samples were heated to temperatures above the isotropization point (85 °C for TDBOSH and TDBOSPyr, 110°C for TDBOSNa) and slowly cooled down to room temperature. During cooling, NMR spectra of the films were recorded.

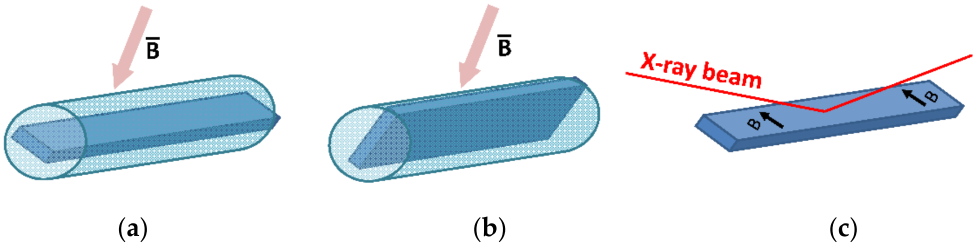

Figure 1. Schematic of the sample orientation in the capillary normal (**a**) and parallel (**b**) to the MF (pink arrow); (**c**) Orientation of X-ray beam in respect to MF direction during GIXD measurements.

The texture of the films after MF exposure was studied using grazing-incidence X-ray diffraction (GIXD) at the BM26 beamline of the European Synchrotron Radiation Facility (Grenoble, France). The measurements were performed at a wavelength of 1.03 Å and the diffraction signal was recorded with a 2D Pilatus 300k detector. The indexation of 2D diffractograms was made using procedures built in IgorPro (Wavemetrics Ltd.) software. For films oriented parallel to the MF, the X-ray beam was oriented normal to the direction of the MF (Figure 1c).

3. Results

The DSC thermograms of the synthesized mesogens TDOBSH, TDOBSNa and TDOBSPyr are presented in Figure 2, and their thermal parameters are summarized in Table 1.

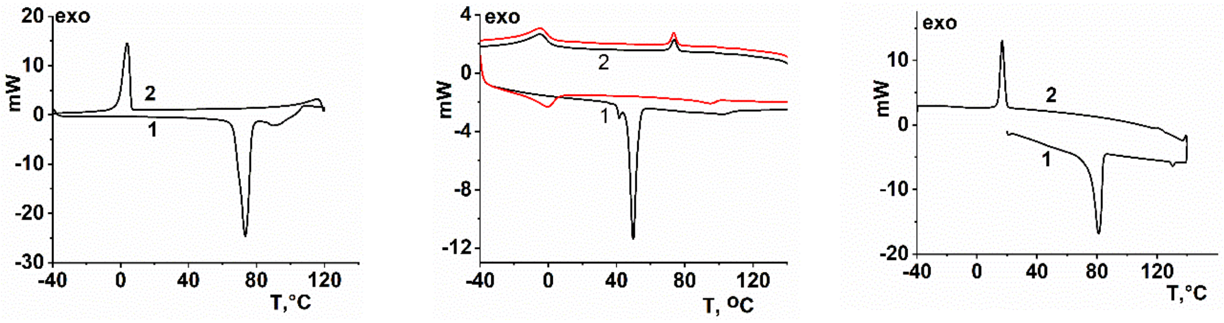

(**a**) (**b**) (**c**)

Figure 2. DSC heating (1) and cooling (2) thermograms for mesogens: (**a**) TDOBSH, (**b**) TDOBSNa (1st cycle—black line, 2nd cycle—red line), (**c**) TDOBSPyr. Exo peaks are positive. Scanning rate 5 °C/min.

Table 1. Thermal parameters of TDOB, TDOBSH, TDOBSNa and TDOBSPyr measured by DSC.

Sample	Heating				Cooling	
	T_1, °C	ΔH, J/g	T_2, °C	ΔH, J/g	T_1, °C	T_2, °C
TDOB	42.9	188.8	-	-	21.5	-
TDOBSH						
1st heating	72.7	99.0	90.0	5.1	-	4.1
2nd heating	6.8	-	17.0	-	10.8	−0.7
TDOBSNa						
1st heating	49.7	46.7	105.0	4.2	73.7	−4.8
2nd heating	−0.7	-	94.0	-	73.6	−4.6
TDOBSPyr						
1st heating	79.7	105.9	128.3	1.7	120.0	17.9

The precursor TDOB has a single endothermic melting peak of the isotropization of the crystalline phase (Table 1), which indicates the absence of LC state. The second endothermic peak both on the first and on the second DSC heating ramps in the region 90–130 °C shows the isotropization of the LC phase (see Figure 2 and Table 1). The values found for the transition temperatures are close to the data that can be found in the literature [3,4,16–22].

To improve the texture of the thin films of the studied sulphonates, the samples were annealed in the temperature window of existence of the LC phase between T_1 and T_2. On one hand, at this temperature, the molecular mobility is enhanced to thermodynamically reach the equilibrium phase and form large ordered domains. On the other hand, the thin films in LC state keep a certain mechanical stability, whereas isotropization can lead to dewetting and other negative factors. As-cast and annealed films were studied using POM. The formation of spherulitic textures typical for crystalline material is observed for the TDOBSH as-cast film (Figure 3a). After the annealing of the films, the birefringence largely disappears indicating either isotropization or the formation of an optically inactive cubic phase (Figure 3b).

The POM image of the as-cast film of sodium salt shows optically active needle-like domains typical of a smectic or columnar LC phase (Figure 3c). Annealing at 85 °C results in the growth of optical activity and the appearance of granular texture (Figure 3d). The presence of bulky pyridinium counterion significantly changes the self-assembly of the thin film. Microphotographs of the as-cast film of TDOBSPyr show a fine-grained structure with low optical activity (Figure 3e). Annealing leads to a decrease in optical density, indicating the formation of a cubic phase (Figure 3f). Thus, depending on the type of counterion and thermal prehistory, the synthesized mesogens reveal a variety of supramolecular structures.

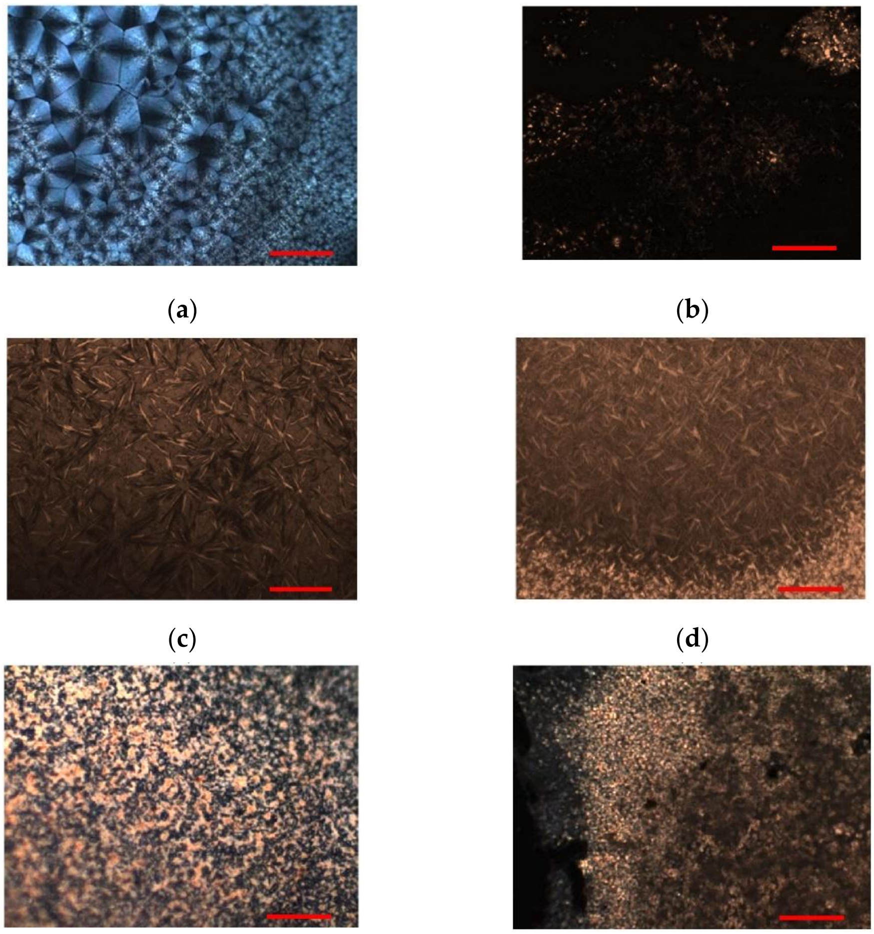

(**a**) (**b**)

(**c**) (**d**)

(**e**) (**f**)

Figure 3. Optical micrographs of films before and after annealing for: TDOBSH (**a**,**b**); TDOBSNa (**c**,**d**); TDOBSPyr (**e**,**f**). The scalebar is 50 mkm.

A detailed analysis of the crystalline and LC structure of the thin films was made using GIXD technique. The investigation of the as-cast thin films of TDOBSH reveals the formation of a smectic structure with lattice parameter a_{sm} = 36.8 Å and a small fraction of gyroid cubic phase with parameter a_{gyr} = 98.0 Å (Figure 4A) [23]. During the annealing of the sample at 85°C, the smectic phase transforms into a thermodynamically stable gyroid structure with decreased parameter a_{gyr} = 98.0 Å (Figure 4B). The GIXD patterns of TDOBSNa indicate the presence of hexagonal columnar phase with parameter a_{hex} = 36.6 Å in both as-cast and annealed films (Figure 4C,D). The increase of half-width of the reflections after annealing indicates a certain growth of grain-like domains without any preferential orientation. The analysis of the GIXD diffractograms of the as-cast films of TDOBSPyr reveals a self-assembly process similar to TDOBSH (Figure 4E,F). During annealing, the smectic phase (a_{sm} = 41.3 Å) transforms into an Im3hm cubic phase with a_p = 48.4 Å. The formation of a primitive cubic phase was detected earlier for wedge-shaped sulfonates with potassium cation at high temperatures [21]. Consequently, the formation of an Im3hm cubic phase in the thin film of TDOBSPyr can be explained by the presence of bulky pyridinium counterions. The results of indexation are summarized in Table 2.

One can see that the variation of the type of counterion allows for the changing thermal and phase behavior of the synthesized mesogens, as well as the topology of ion channels. The existence of a liquid-crystalline state at an elevated temperature can be explained by the disordering of linear alkyl chains and the increase in the local molecular mobility [8]. However, for the practical application of synthesized compounds as proton-conductive membranes, it is important to ensure the homeotropic orientation of water channels in the columnar and smectic phases. After the formation of such a thermodynamically metastable state at an elevated temperature, the orientation can be consequently fixed by the crystallization of the mesogens while they cool to room temperature, without disturbing the supramolecular organization. The most effective external stimulus for forming a metastable homeotropic LC texture is the application of a strong magnetic field assessable in an NMR spectrometer.

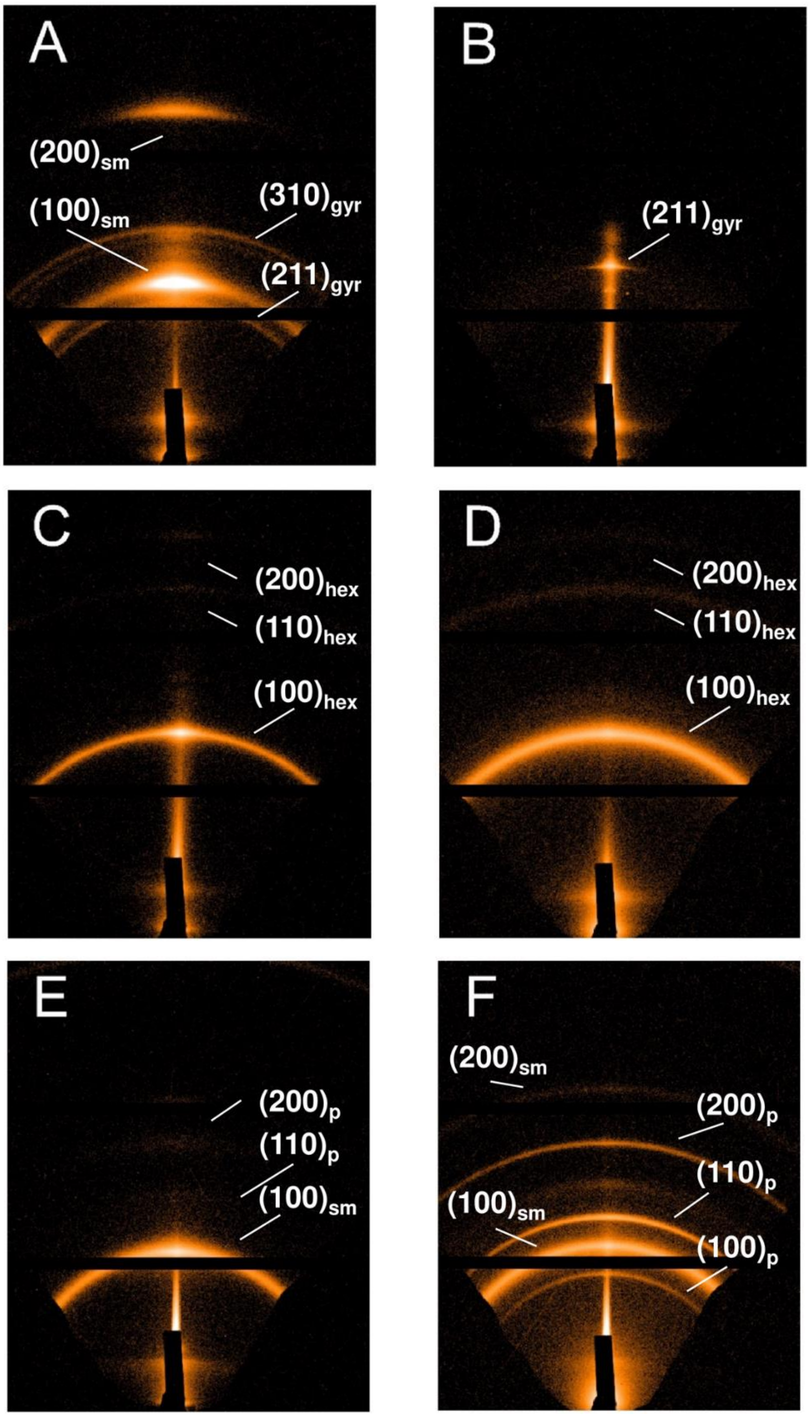

Figure 4. 2D GIXD patterns of TDOBSH (**A**,**B**), TDOBSNa (**C**,**D**) and TDOBSPyr (**E**,**F**) before (**A**,**C**,**E**) and after (**B**,**D**,**F**) annealing. The most intense reflections are marked with white arrows and indexed according to smectic (sm), gyroid (gyr), columnar hexagonal (hex) and cubic primitive (p) phases. The film was oriented horizontally. The black regions appear after background substruction.

Table 2. Indexation of GIXD patterns of thin films.

Sample	As-Cast Films			After Annealing		
	Phase	hkl	d_{exp}, Å	Phase	hkl	d_{exp}, Å
TDOBSH	Sm a_{sm} = 36.9 Å	100	36.9	Cub_{gyr} a_{gyr} = 93.2 Å	211	37.9
		200	18.6		220	33.3
	Cub_{gyr} a_{gyr} = 98.0 Å	211	41.4		310	29.3
		310	29.9			
		222	28.2			
TDOBSPyr	Sm a_{sm} = 41.3 Å	100	41.3	Sm a_{sm} = 40.0 Å	100	40.0
		200	20.7		200	20.0
		300	13.9		300	13.3
	Cub_p a_p = 48.4 Å	200	24.2	Cub_p a_p = 48.5 Å	100	48.4
					110	33.9
					111	29.0
					200	24.2
TDOBSNa	Col_h a_{hex} = 36.6 Å	100	31.7	Col_h a_{hex} = 36.2 Å	100	31.5
		110	18.4		110	18.3
		200	15.9		200	15.6

Figure 5 shows NMR spectra of synthesized mesogens in LC state obtained at different temperatures on a BRUKER 500 spectrometer with a proton frequency of 500 MHz. The narrow line at ~1 ppm on the NMR spectra of TDOBSH corresponds to acid protons (Figure 5a). A similar peak is visible for TDOBSNa, indicating the formation of a crystalline hydrate with one water molecule (Figure 5b). The variation of the structure was detected only after allowing the mesogens to cool to 24 °C. The narrow peak in Figure 5c corresponds to the hydrogen bonding of the mesogen and pyridinium proton of TDOBSHPyr. As expected, the intensity of this line increases during heating, indicating the self-assembly of the material.

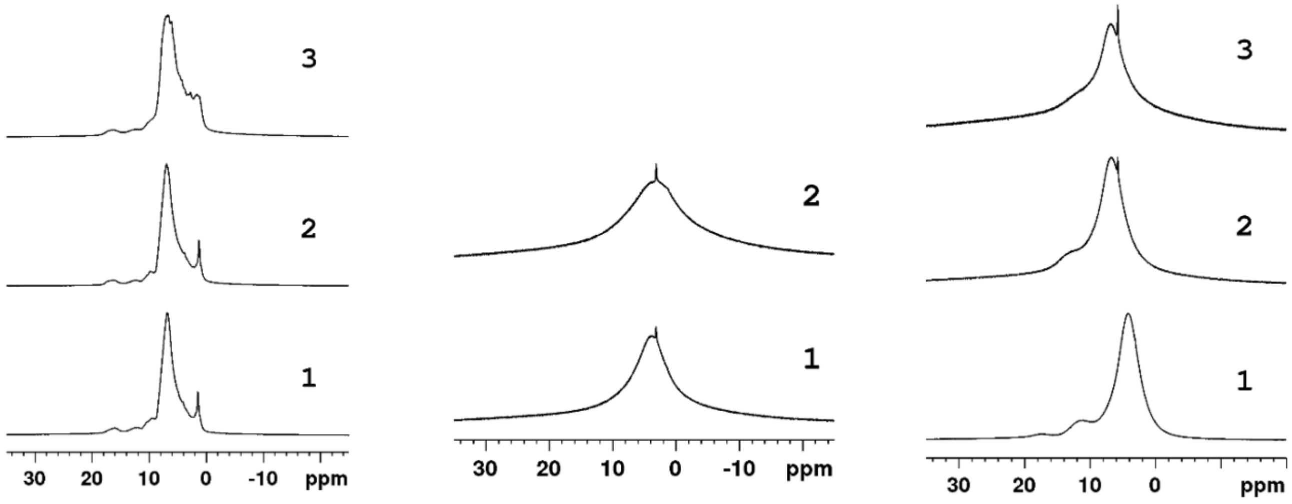

(a) (b) (c)

Figure 5. NMR spectra of synthesized mesogens: (**a**)—TDOBSH at 80 °C (1), 50 °C (2) and 30 °C (3); (**b**)—TDOBSNa at 80 °C (1), 24 °C (2); (**c**)—TDOBSPyr at 80 °C (1), 50 °C (2), 30 °C (3).

The effect of the magnetic field on the thin films' texture was studied via GIXD using a synchrotron source. Figure 6A–C shows 2D GIXD diffractograms for the TDOBSH thin film before and after the MF. The application of the MF parallel to the film surface results in the orientation of the initially isotropic gyroid cubic phase and the appearance of a small fraction of the smectic phase (Figure 6B). For the gyroid lattice, the 211 vector is oriented normal to the substrate. For the normal orientation of the MF, the GIXD pattern demonstrates two weak meridional reflections of the gyroid phase (Figure 6C). Consequently, parallel alignment of the MF stimulates the development of large, well-oriented domains of the cubic phase. For sodium salt, we did not observe significant changes in the hexagonal phase texture after the application of the MF parallel to the film compared to the non-exposed annealed sample (Figure 6D,E). However, the normal orientation of the MF causes a degree of disorientation to the hexagonal phase and the appearance of a weak peak in the small-angle region, which can be attributed to the less stable smectic phase (Figure 6F). Thus, the normal orientation of the MF prevents the formation of large regular domains of the columnar hexagonal mesophase. For pyridinium salt, the self-assembly of mesogens with the MF parallel to the film leads to a partial transformation of the initial oriented primitive cubic phase into the smectic phase (Figure 6G,H). In contrast, having the MF oriented normal to the film stimulates the formation of a mixture of unoriented and well-oriented primitive Im3hm cubic phase with 100 vector oriented normal to the surface (Figure 6I). The difference in the effect of the MF orientation on the texture improvement for TDOBSPyr can be explained by the interaction of the MF with the pyridinium rings.

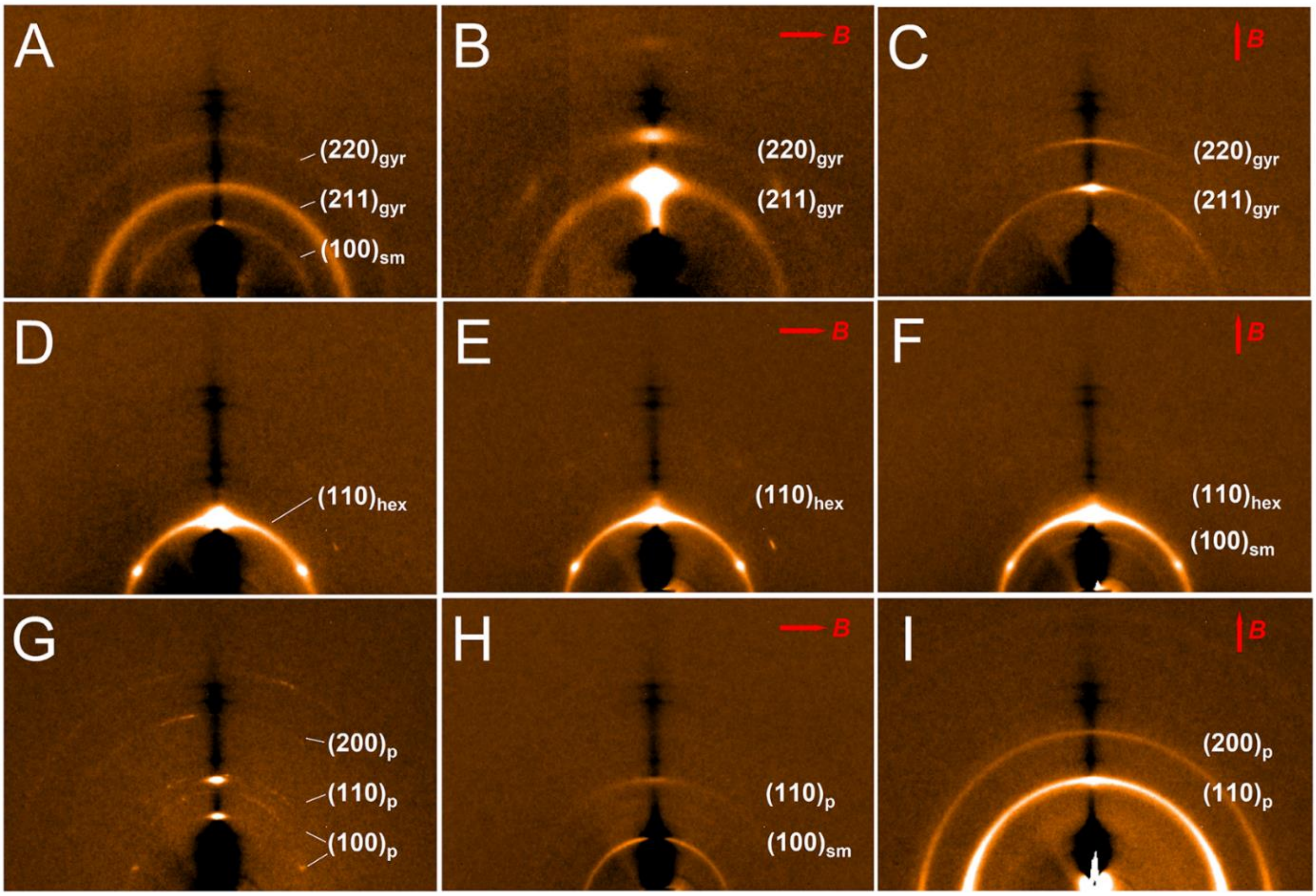

Figure 6. 2D GIXD patterns of TDOBSH (**A**–**C**), TDOBSNa (**D**–**F**) and TDOBSPyr (**G**–**I**): left column – before application of MF, middle column—with MF parallel to the film, right column—with MF normal to the film. The most intense reflections are marked with white arrows and indexed according to smectic (sm), gyroid (gyr), columnar hexagonal (hex) and cubic primitive (p) phases. The film was oriented horizontally. Red arrow indicates direction of magnetic field with respect to the film surface. The black regions appear after background substruction.

The diffractograms presented confirm the ability of the magnetic field to affect the texture and degree of the ordering of amphiphilic mesogens. The largest effect of the magnetic field is observed for the pyridine salt, which can probably be explained by the weak ordering of the mesogen molecules in the initial film and the magnetic susceptibility of the pyridinium. A fraction of highly ordered primitive cubic phase is formed as a result of MF exposure. For the acid, on the other hand, a decrease in the initial cubic phase is observed, possibly due to the rapid cooling of the sample in the NMR instrument. For the highly ordered columnar phase of the sodium salt, the effect of the MF application in both directions is minimal.

4. Conclusions

In this work, the reorganization of the texture of thin liquid-crystalline films in a smectic state was shown for the first time. It is noteworthy that the field-induced texture is metastable without the magnetic field (MF) but can be fixed thanks to the ability of the compounds to crystallize at room temperature and thereby create a physical network of crystalline domains. To this end, we synthesized derivatives of a wedge-shaped amphiphilic mesogen—asymmetric 2,3,4-tris(dodecyloxy)benzenesulfonate and its pyridine and sodium salts. The processes of the self-assembly of the synthesized mesogens in bulk and in thin films were preliminarily studied using DSC, POM and GIXD. The influence of an MF oriented along or normal to the film surface on the supramolecular structure formation at different temperatures was studied. It was found that depending on the counterion nature, the samples demonstrate specific thermotropic behavior and form different supramolecular structures. For thin films of TDOBSH, high-temperature annealing results in the transition from a metastable smectic LC phase to a cubic bicontinuous gyroid phase. Applying an MF parallel to the film surface stimulates the alignment of the cubic domains. In contrast, the orientation of the MF normal to the substrate hinders the growth of the regular domains of the gyroid phase during slow cooling from the LC state to room temperature. The sodium salt (TDOBSNa) exhibits the formation of a columnar hexagonal LC phase irrespective of the thermal history. We speculate that the application of the MF along the normal direction slightly hinders the growth of large columnar domains due to the appearance of a metastable smectic phase.

Among all the studied molecules the most pronounced effect of the MF on self-assembly was detected for the pyridinium salt. The stable Im3hm cubic phase which forms during annealing completely disappears under the action of the MF oriented along the TDOBSPyr film. The realignment of the mesogens results in the appearance of the smectic phase typical of the as-cast films. In contrast, the normally oriented MF improves the development of large, highly oriented domains of the Im3hm cubic phase during cooling. The reason for the specific behavior of TDOBSPyr in the MF could be due to the anisotropy of the magnetic susceptibility of pyridine. The obtained results can help with the development of strategies for the fabrication of novel proton-conductive membranes built with a "bottom-up" approach.

Author Contributions: Conceptualization, D.V.A.; data curation, A.F.A.; formal analysis, K.N.G.; investigation, E.S.P.; methodology, V.P.T.; supervision, D.V.A.; writing—original draft preparation, L.L.G.; writing—review and editing, D.A.I. All authors have read and agreed to the published version of the manuscript.

Funding: The synthetic part of the work was funded by State orders No. 0089-2019-0012 (state registration number AAA-A19-119032690060-9) and No. 0089-2019-0002 (state registration number AAA-A19-119071190017-7). The structural characterization of the phases and orientation was funded by the Sirius University of Science and Technology.

Institutional Review Board Statement: Not applicable.

Informed Consent Statement: Not applicable.

Data Availability Statement: The data presented in this study are available in article.

Acknowledgments: The authors thank the IPCP RAS Analytical Center for the ^{1}H and ^{13}C NMR tests and for the elemental analysis and M. Rosenthal (BM26, ESRF) for GIXD experiments.

Conflicts of Interest: The authors declare no conflict of interest.

References

1. Antipin, I.S.; Alémov, M.V.; Arslanov, V.V.; Burilov, V.A.; Vatsadze, S.Z.; Voloshin, Y.Z.; Volcho, K.P.; Gorbatchuk, V.V.; Gorbunova, Y.G.; Gromov, S.P.; et al. Functional supramolecular systems: Design and applications. *Russ. Chem. Rev.* **2021**, *90*, 895–1107. [CrossRef]
2. Alfutimie, A.; Curtis, R.; Tiddy, G.J.T. Lyotropic Surfactant Liquid Crystals: Micellar Systems. In *Handbook of Liquid Crystals*, 2nd ed.; Goodby, J., Collings, P., Kato, T., Tschierske, C., Gleeson, H., Raynes, P., Vill, V., Eds.; Wiley-VCH: Weinheim, Germany, 2014; Volume 6.
3. Li, L.; Rosenthal, M.; Zhang, H.; Hernandez, J.; Drechsler, M.; Phan, K.H.; Rütten, S.; Zhu, X.; Ivanov, D.A.; Möller, M. Light-Switchable Vesicles from Liquid-Crystalline Homopolymer-Surfactant Complexes. *Angew. Chem. Int.* **2012**, *51*, 11616–11619. [CrossRef]
4. Zhang, H.; Li, L.; Möller, M.; Zhu, X.; Hernandez, J.; Rueda, J.; Rosenthal, M.; Ivanov, D.A. From Channel-Forming Ionic Liquid Crystals Exhibiting Humidity-Induced Phase Transitions to Nanostructured Ion-Conducting Polymer Membranes. *Adv. Mater.* **2013**, *25*, 3543–3548. [CrossRef] [PubMed]
5. Mauritz, K.A.; Moore, R.B. State of Understanding of Nafion. *Chem. Rev.* **2004**, *104*, 4535–4586. [CrossRef] [PubMed]
6. Allison, S.A.; Barrer, R.M. Sorption in the β-phases of transition metal(II) tetra-(4-methylpyridine) thiocyanates and related compounds. *J. Chem. Soc. A* **1969**, *17*, 17–23. [CrossRef]
7. Barrer, R.M.; Galabova, I.M. Ion-Exchanged Forms of Zeolite L, Erionite, and Offretite and Sorption of Inert Gases. *Adv. Chem. Ser.* **1973**, *121*, 1–28.
8. Grafskaia, K.N.; Anokhin, D.V.; Zimka, B.I.; Izdelieva, I.A.; Zhu, X.; Ivanov, D.A. An "on–off" switchable cubic phase with exceptional thermal stability and water sorption capacity. *Chem. Commun.* **2017**, *53*, 13217–13220. [CrossRef]
9. Sirringhaus, H.; Brown, P.J.; Friend, R.H.; Neilsen, M.M.; Bechgaard, K.; Langeveld-Voss, B.M.W.; Spiering, A.J.H.; Janssen, R.A.J.; Meijer, E.W.; Herwig, P.; et al. Two-dimensional charge transport in self-organized, high-mobility conjugated polymers. *Nature* **1999**, *401*, 685–688. [CrossRef]
10. Hosono, N.; Kajitani, T.; Fukushima, T.; Ito, K.; Sasaki, S.; Takata, M.; Aida, T. Large-Area Three-Dimensional Molecular Ordering of a Polymer Brush by One-Step Processing. *Science* **2010**, *330*, 808–811. [CrossRef]
11. Grelet, E.; Bock, H. Control of the orientation of thin open supported columnar liquid crystal films by the kinetics of growth. *Europhys. Lett.* **2006**, *73*, 712–718. [CrossRef]
12. Majewski, P.W.; Gopinadhan, M.; Jang, W.S.; Lutkenhaus, J.L.; Osuji, C.O. Anisotropic Ionic Conductivity in Block Copolymer Membranes by Magnetic Field Alignment. *J. Am. Chem. Soc.* **2010**, *132*, 17516–17522. [CrossRef] [PubMed]
13. Tousley, M.E.; Feng, X.; Elimelech, M.; Osuji, C.O. Aligned Nanostructured Polymers by Magnetic-Field-Directed Self-Assembly of a Polymerizable Lyotropic Mesophase. *ACS Appl. Mater. Interfaces* **2014**, *6*, 19710–19717. [CrossRef] [PubMed]
14. Vita, F.; Hegde, M.; Portale, G.; Bras, W.; Ferrero, C.; Samulski, E.T.; Francescangeli, O.; Dingemans, T. Molecular ordering in the high-temperature nematic phase of an all-aromatic liquid crystal. *Soft Matter* **2016**, *12*, 2309–2314. [CrossRef] [PubMed]
15. Feng, X.; Tousley, M.E.; Cowan, M.G.; Wiesenauer, B.R.; Nejati, S.; Choo, Y.; Noble, R.D.; Elimelech, M.; Gin, D.L.; Osuji, C.O. Scalable Fabrication of Polymer Membranes with Vertically Aligned 1 nm Pores by Magnetic Field Directed Self-Assembly. *ACS Nano* **2014**, *8*, 11977–11986. [CrossRef]
16. Zhu, X.; Tartsch, B.; Beginn, U.; Möller, M. Wedge-Shaped Molecules with a Sulfonate Group at the Tip—A New Class of Self-Assembling Amphiphiles. *Chem. Eur. J.* **2014**, *10*, 11977–11986. [CrossRef]
17. Pifferi, G.; Monguzzi, R. New compounds: Synthesis of 3,4,5-trimethoxybenzenesulfonamides. *J. Pharm. Sci.* **1973**, *63*, 1392–1394. [CrossRef]
18. Zhu, X.; Beginn, U.; Möller, M.; Gearba, R.I.; Anokhin, D.V.; Ivanov, D.A. Self-Organization of Polybases Neutralized with Mesogenic Wedge-Shaped Sulfonic Acid Molecules: An Approach toward Supramolecular Cylinders. *J. Am. Chem. Soc.* **2006**, *128*, 16928–16937. [CrossRef]
19. Zhu, X.; Scherbina, M.A.; Bakirov, A.V.; Gorzolnik, B.; Chvalun, S.N.; Beginn, U.; Moeller, M. Methacrylated Self-Organizing 2,3,4-Tris(alkoxy)benzenesulfonate: A New Concept Toward Ion-Selective Membranes. *Chem. Mater.* **2006**, *18*, 4667–4673. [CrossRef]
20. Beginn, U.; Yan, L.; Chvalun, S.N.; Shcherbina, M.A.; Bakirov, A.; Moeller, M. Thermotropic columnar mesophases of wedge-shaped benzenesulfonic acid mesogens. *Liq. Cryst.* **2008**, *35*, 1073–1093. [CrossRef]
21. Shcherbina, M.A.; Bakirov, A.V.; Yakunin, A.N.; Beginn, U.; Yan, L.; Moeller, M.; Chvalun, S.N. The effect of the shape of the mesogenic group on the structure and phase behavior of 2,3,4-tris(dodecyloxy)benzenesulfonates with alkaline cations. *Soft Matter* **2014**, *10*, 1746–1757. [CrossRef]

22. Shcherbina, M.A.; Bakirov, A.V.; Yan, L.; Beginn, U.; Zhu, X.; Moeller, M.; Chvalun, S.N. Heuristics for precise supramolecular control of soft matter structure and properties–2,3,4-tris(dodecyloxy)benzenesulfonates with alkaline and organic cations. *Mendeleev Commun.* **2015**, *5*, 142–144. [CrossRef]
23. Garstecki, P.; Holyst, R. Scattering Patterns of Multiply Continuous Cubic Phases in Block Copolymers. I. The Model. *Macromolecules* **2003**, *36*, 9181–9190. [CrossRef]